Effect of electron transport layer crystallinity on the transient characteristics of inverted organic solar cells

Yong-Jin Kang,[1,2] Chang Su Kim,[1,a)] Dae Sung You,[1] Sung Hoon Jung,[1] Kyounga Lim,[1] Do-Geun Kim,[1] Jong-Kuk Kim,[1] Soo Hyung Kim,[2] Yu-Ri Shin,[3] Se-Hun Kwon,[3,b)] and Jae-Wook Kang[1,c)]

[1]*Department of Material Processing, Korea Institute of Materials Science, Changwon 641-831, South Korea*
[2]*Department of Nano Fusion Technology, Pusan National University, Busan 609-735, South Korea*
[3]*National Core Research Center for Hybrid Materials Solution, Pusan National University, Busan 609-735, South Korea*

(Received 8 June 2011; accepted 31 July 2011; published online 19 August 2011)

We present how the crystallinity of the electron transport layer can dramatically influence the transient characteristics of organic solar cells. We employed an inverted cell structure using TiO_x prepared by atomic layer deposition as an electron transport layer. The device possessing the amorphous phase TiO_x exhibited a continuous increase in the device characteristics upon continuous illumination at ambient, which is attributed to the filling of shallow electron traps within the amorphous phase TiO_x upon illumination. In contrast, the characteristics of the device with the crystalline phase TiO_x showed a negligible increase upon continuous illumination. © *2011 American Institute of Physics*. [doi:10.1063/1.3628319]

Organic solar cells (OSCs) are potential candidates in the solar energy harvesting industry. These devices offer a renewable, sustainable energy source and have a low-cost fabrication and mechanical flexibility.[1,2] Conventional OSC devices are usually based on the following layer sequence: indium tin oxide (ITO)/poly(3,4-ethylene dioxythiophene doped with polystyrene sulfonate) (PEDOT:PSS)/active layer/metal electrode with low work function.[3,4] However, low work function metals, such as Al and Ca, can oxidize during exposure to ambient conditions; the resulting oxide layer has been shown to produce an insulating barrier that reduces the conductivity of the electrode, effectively increasing the serial resistance of the device. In addition, the deposition of these metals can lead to metal migration through the active layer, which can react with the polymer and alter its semiconducting properties.[5,6] Furthermore, the ITO/PEDOT:PSS interface is known to be rather chemically and morphologically unstable.[7,8] Although power conversion efficiencies of up to 7% have been reported for these conventional OSCs, this type of conventional device has proved to be very unstable; its efficiency was reduced to less than half of its original value after one day of storage and totally degraded after four days.[9] Considerable improvement in the device stability under normal operating conditions needs to be achieved.

For this reason, an OSC device with an inverted geometry has been proposed. An inverted OSC typically uses a metal oxide (ZnO or TiO_x) for the bottom contact, and more air-stable high work function metals such as Au for the top electrode.[10–12] Although these devices show reasonable efficiencies of almost 3% and 4%, these transient photovoltaic behavior results were not obtained under continuous illumination in air over a real time evaluation of the device performance under normal environmental conditions. The transient photovoltaic behavior of OSCs needs to be acquired for real-life applications and the understanding and improvement of the environmental stability are a prerequisite.[13,14]

In this paper, we present a study on how the crystallinity of the electron transport layer can dramatically influence the transient characteristics of an inverted OSC. We employed an inverted cell structure using TiO_x prepared by atomic layer deposition (ALD) as an electron transport layer. Due to the self-limiting characteristic of the reaction between the reactant gas and a solid surface, conformal and pin-hole-free TiO_x films can be deposited layer by layer on an atomic scale.[15]

The inverted OSC structure is shown in Fig. 1(a). TiO_x films were deposited on the indium-tin-oxide (ITO)-coated substrate by ALD at a deposition temperature of 220 °C and a pressure of 1 Torr using titanium isopropoxide (TTIP, Mecharonics Co. Ltd) as the titanium precursor and H_2O vapor as the oxygen reactant. The poly(3-hexylthiophene) (P3HT):[6,6]-phehyl-C_{61} butyric acid methyl ester (PCBM) blend film was spin-coated onto the TiO_x layer in a glove box. A buffer layer of PEDOT-PSS was spin-coated onto the P3HT:PCBM layer with a thickness of approximately 40 nm. Finally, a 120-nm-thick Ag electrode was evaporated onto the PEDOT:PSS layer through a shadow mask, which defined the effective area at 0.38 cm^2. The current voltage (*J-V*) characteristics were measured using a Keithley 2400 source meter under either dark conditions or at a 100 mW/cm^2 (AM 1.5 G) irradiation from a solar simulator.

Figure 1(b) shows the *J-V* characteristics of the inverted OSC employing 10 and 20 nm thick TiO_x acquired after 20 min of continuous illumination under 100 mW/cm^2. The 10 nm TiO_x device exhibited a power conversion efficiency of 1.89%, with a fill factor (FF) of 40%. The short-current density (J_{sc}) and the open-circuit voltage (V_{oc}) were 8.65 mA/cm^2 and 0.54 V, respectively. However, the 20 nm TiO_x device exhibited a power conversion efficiency of 3.09% with

a)Electronic mail: changsu1025@kims.re.kr.
b)Electronic mail: sehun@pusan.ac.kr.
c)Electronic mail: jwkang@kims.re.kr.

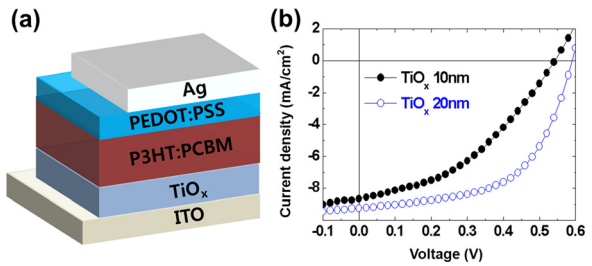

FIG. 1. (Color online) (a) Schematic diagram of the inverted organic solar cell configuration incorporating TiO_x as the electron transport layer and (b) *J-V* characteristics of the devices employing 10 and 20 nm TiO_x films.

a $J_{sc} = 9.24$ mA/cm^2, a $V_{oc} = 0.59$ V, and an FF = 56%. It is thought that in the thicker TiO_x device, the collection of electrons to the ITO cathode is further enhanced by a continued reduction of the bulk electric field.[15]

Figure 2 summarizes the performance parameters of the device under illumination. The devices were tested immediately after the Ag evaporation and their *J-V* characteristics were acquired every minute thereafter under continuous illumination. The *J-V* characteristics of a representative 10 nm TiO_x device are shown in Fig. 2(a). The device characteristics improve under continuous illumination and saturate after 20 min. Unlike the 10 nm TiO_x device, the photovoltaic behavior of the 20 nm TiO_x device does not change significantly under extended illumination. A comparison of the device characteristics shown in Fig. 2 implicates the thickness of TiO_x layer as being responsible for the transient photovoltaic behavior observed in our inverted organic solar cells. Like other metal oxides, the conductivity of TiO_x is sensitive to light exposure since illumination can lead to the direct excitation of electrons from the valence band to the conduction band.[16–18] These initially excited electrons must fill the shallow electron traps that are present in the TiO_x conduction band; the photoconductivity of the TiO_x, therefore, increases under continuous illumination and saturates when all of the shallow electron traps are filled. We, therefore, attribute the improvement in the device characteristics seen in Fig. 2(a) to the filling of the shallow electron traps in the TiO_x. Increasing the photoconductivity of the TiO_x reduces the serial resistance in our inverted OSC.[19] This reduction in serial resistance increases the J_{SC} and is directly manifested in the evolution of the shape of the *J-V* curves. It also reduces the energetic losses at the photo-active layer/ITO interface, thereby dramatically increasing the J_{SC} and V_{OC}. Given that all the devices were prepared in one batch, the TiO_x trap density in these devices must be comparable.

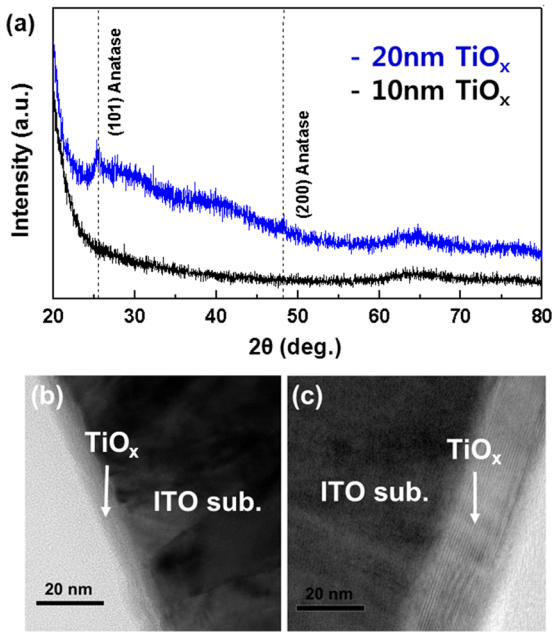

FIG. 3. (Color online) (a) XRD patterns of TiO_x films depending on the film thickness. HRTEM images of (b) 10 nm and (c) 20 nm TiO_x films deposited on the ITO substrate.

The effect of the film thickness on the crystallinity of the as deposited TiO_x films was investigated through XRD and HRTEM analysis. Figure 3(a) shows the XRD patterns of the 10 nm and 20 nm thick as deposited TiO_x films. The 10 nm films showed no clear peaks, indicating that the film had an amorphous structure. The 20 nm films had clear peaks, indicating that they were well-crystallized. Referring to the joint committee for powder diffraction standards (JCPDS) files, the crystallinity of TiO_x is identified as an anatase TiO_x. It is generally agreed that TiO_x films grown by ALD using TTIP show a thickness-dependent crystallization behavior.[20] TiO_2 films maintain an amorphous structure up to a certain critical thickness; the films spontaneously crystallize above the critical film thickness. The critical thickness point increases with a decrease in the TiO_x growth temperature. In our results, therefore, the critical thickness for the amorphous-crystallization transition appears to be higher than 10 nm; the TiO_x films having a lower thickness than 20 nm remained amorphous. Figures 3(b) and 3(c) show the HRTEM images of the 10 nm and 20 nm TiO_x films deposited on the ITO substrate. From the cross-sectional HRTEM image, the TiO_x film was uniformly deposited on the ITO substrate by the ALD technique without showing any

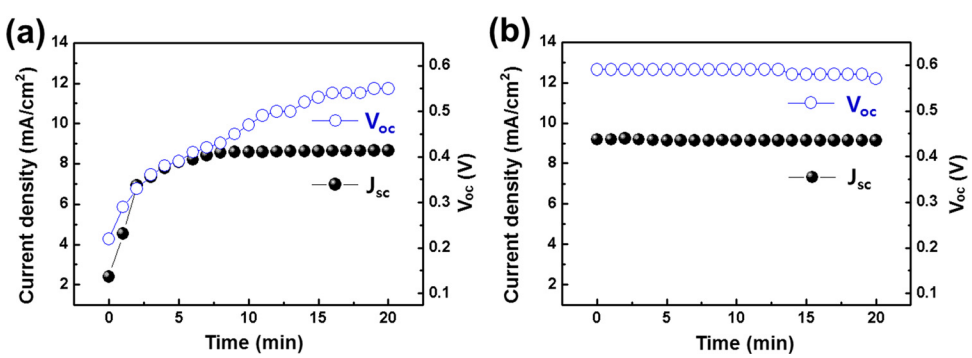

FIG. 2. (Color online) Illumination time dependence of the short circuit current J_{SC} and the open circuit voltage V_{OC} for the inverted organic solar cells employing (a) 10 nm and (b) 20 nm TiO_x films.

pin-holes. Similar to the XRD results, the HRTEM image of the 10 nm TiO_x shows that the film had an amorphous structure, whereas the 20 nm TiO_x film was well–crystallized as seen in the lattice fringes in the HRTEM image in Figure 3(c). The devices possessing the amorphous phase TiO_x exhibited a continuous increase in their device characteristics upon continuous illumination at ambient, which is attributed to the filling of the shallow electron traps within the amorphous phase TiO_x upon illumination. In contrast, the characteristics of the crystalline phase TiO_x devices show negligible increases upon continuous illumination.

In summary, we have fabricated inverted OSC utilizing a ALD processed TiO_x electron transport layer between the ITO and the active layer and Ag as a back hole collecting electrode. We investigated into how the crystallinity of the electron transport layer can dramatically influence the transient characteristics of organic solar cells. The observed distinct crystallinity-dependent device characteristics reflect that optimizing the film crystallinity of the electron transport layer might lead to the development of more efficient and stable organic solar cells.

[1]Y. Yuan, T. J. Reece, P. Sharma, S. Poddar, S. Ducharme, A. Gruverman, Y. Yang, and J. Huang, Nature Mater. **10**, 296 (2011).
[2]A. Tada, Y. Geng, Q. Wei, K. Hashimoto, and K. Tajima, Nature Mater. **10**, 450 (2011).
[3]D.W. Zhao, S. T. Tan, L. Ke, P. Liu, A. K. K. Kyaw, X. W. Sun, G. Q. Lo, and D. L. Kwong, Sol. Energy Mater. Sol. Cells **94**, 985 (2010).
[4]A. J. Morfa, K. L. Rowlen, T. H. Reilly, M. J. Romero, and J. Lagemaat, Appl. Phys. Lett. **92**, 013504 (2008).
[5]D. E. Gallardo, C. Bertoni, S. Dunn, N. Gaponik, and A. Eychmuller, Adv. Mater. **19**, 3364 (2007).
[6]F. C. Krebs and H. Spanggaard, Chem. Mater. **17**, 5235 (2005).
[7]M. P. de Jong, L. J. van Ijzendoom, and M. J. A. de Voigt, Appl. Phys. Lett. **77**, 2255 (2000).
[8]K. Kawano, R. Pacios, D. Poplavskyy, J. Nelson, D. D. C. Bradley, and J. R. Durrant, Sol. Energy Mater. Sol. Cells **90**, 3520 (2006).
[9]S. K. Hau, H. L. Yip, N. S. Baek, J. Zou, K. O. Malley, and A. K. Y. Jen, Appl. Phys. Lett. **92**, 253301 (2008).
[10]M. S. White, D. C. Olson, S. E. Shaheen, N. Kopidakis, and D. S. Ginley, Appl. Phys. Lett. **89**, 143517 (2006).
[11]C. Waldauf, M. Morana, P. Denk, P. Schilinsky, K. Coakley, S. A. Choulis, and C. J. Brabec, Appl. Phys. Lett. **89**, 233517 (2006).
[12]R. Steim, S. A. Choulis, P. Schilinsky, and C. J. Brabec, Appl. Phys. Lett. **92**, 093303 (2008).
[13]M. Jorgensen, K. Norrman, and F. C. Krebs, Sol. Energy Mater. Sol. Cells **92**, 686 (2008).
[14]M. O. Reese, A. J. Morfa, M. S. White, N. Kopidakis, S. E. Shaheen, G. Rumbles, and D. S. Ginley, Sol. Energy Mater. Sol. Cells **92**, 746 (2008).
[15]J. C. Wang, W. T. Weng, M. Y. Tsai, M. K. Lee, S. F. Horng, T. P. Perng, C. Ch. Kei, C. C. Yu, and H. F. Meng, J. Mater. Chem. **20**, 862 (2010).
[16]K. Pomoni, A. Vomvas, and C. Trapalis, Thin Solid Films **479**, 160 (2005).
[17]P. A. C. Quist, W. J. E. Beek, M. M. Wienk, R. A. J. Janssen, T. J. Savenije, and L. D. A. Siebbeles, J. Phys. Chem. B **110**, 10315 (2006).
[18]T. Kuwabara, T. Nakayama, K. Uozumi, T. Yamaguchi, and K. Takahashi, Sol. Energy Mater. Sol. Cells **92**, 1476 (2008).
[19]C. S. Kim, S. S. Lee, E. D. Gomez, J. B. Kim, and Y. L. Loo, Appl. Phys. Lett. **94**, 113302 (2009).
[20]S. K. Kim, S. Han, J. H. Han, and C. S. Hwang, Appl. Surf. Sci. **257**, 4302 (2011).